Supplement of Nat. Hazards Earth Syst. Sci., 21, 2791–2810, 2021
https://doi.org/10.5194/nhess-21-2791-2021-supplement

Natural Hazards and Earth System Sciences
Open Access
EGU

Supplement of

Multi-decadal geomorphic changes of a low-angle valley glacier in the East Kunlun Mountains: remote sensing observations and detachment hazard assessment

Xiaowen Wang et al.

Correspondence to: Xiaowen Wang (insarwxw@swjtu.edu.cn)

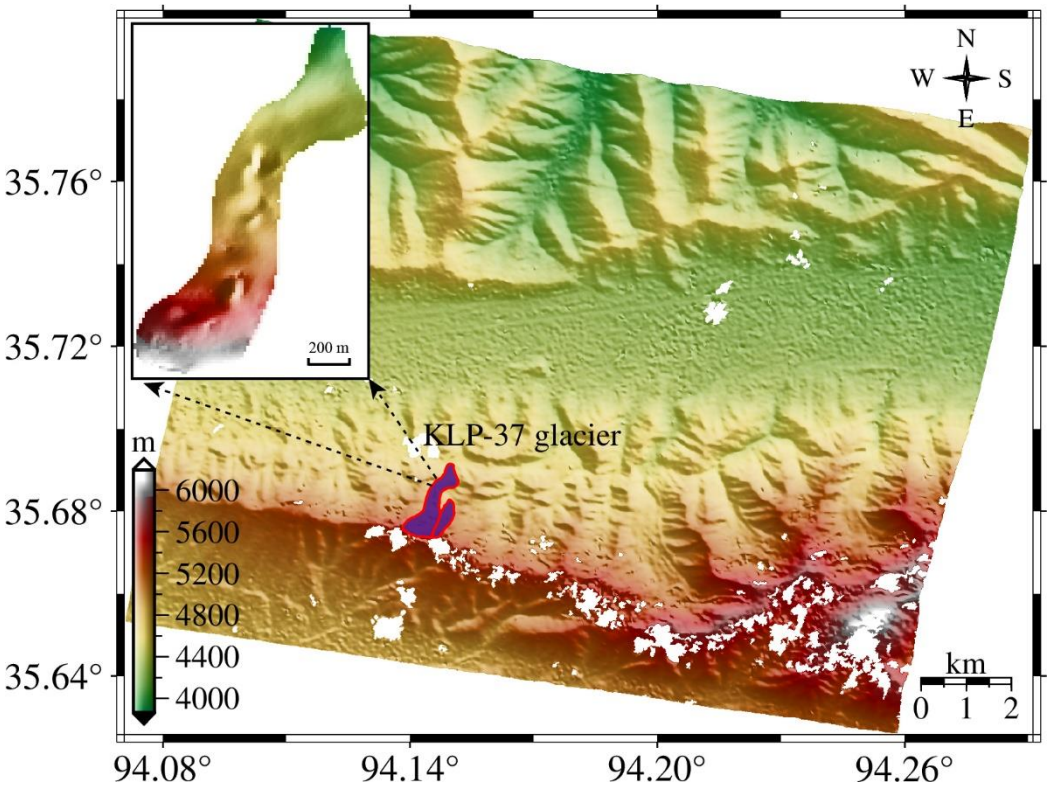

Figure S1: The KH-9 DEM generated from the Hexagon KH-9 stereo images. The inset shows the topography of the KLP-37 glacier.

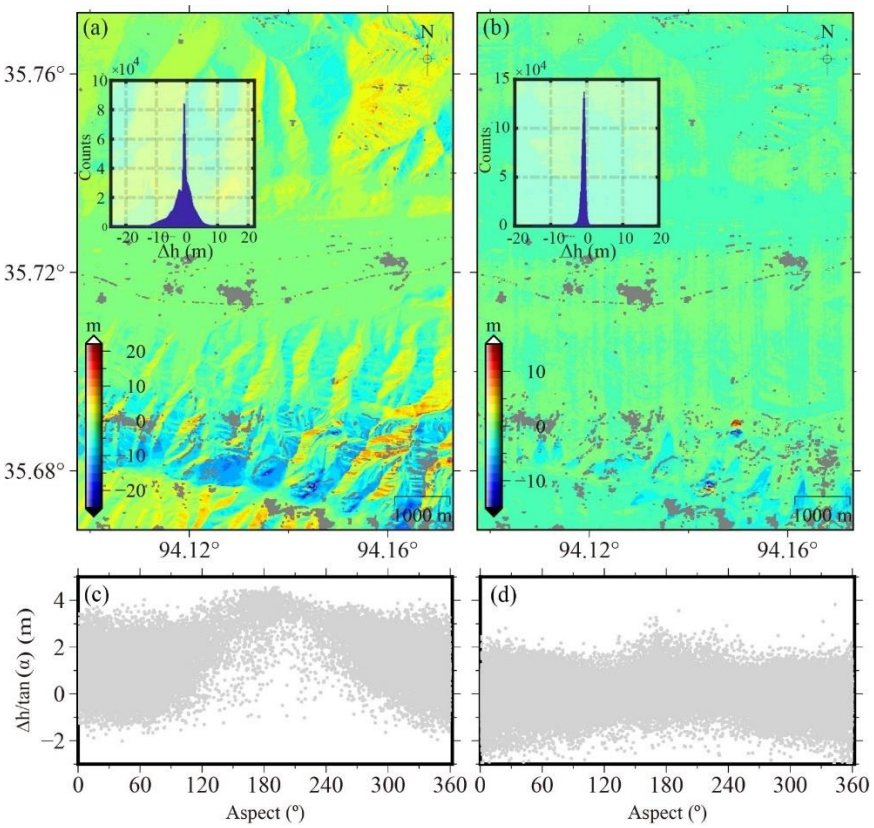

Figure S2: Comparison of DEM differences before (a) and after (b) co-registration. The inset histograms exhibit distributions of DEM differences. (c) and (d) exhibit the plots of $\Delta h/\tan(\alpha)$ against aspect angle before and after the co-registration, and α represents the slope angle.

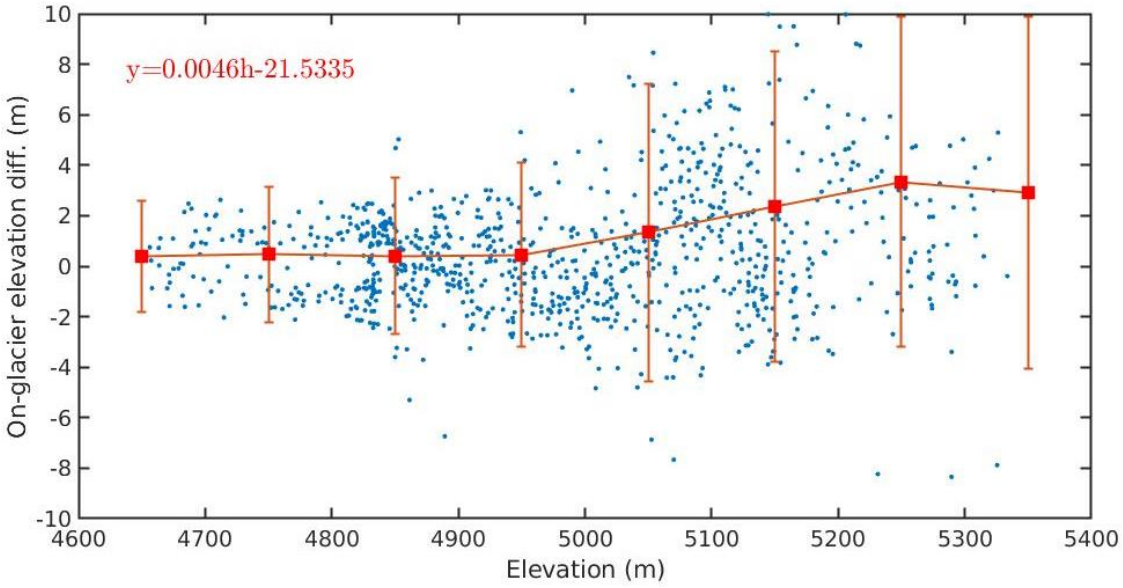

15

Fig. S3: Plot of surface elevation difference between SRTM C-band and X-band DEMs against elevation. The red squares indicate mean values of elevation differences for elevation bins with a 100 m separation. The correction model *y*=0.046*h*-21.5335 was obtained from linear fitting.

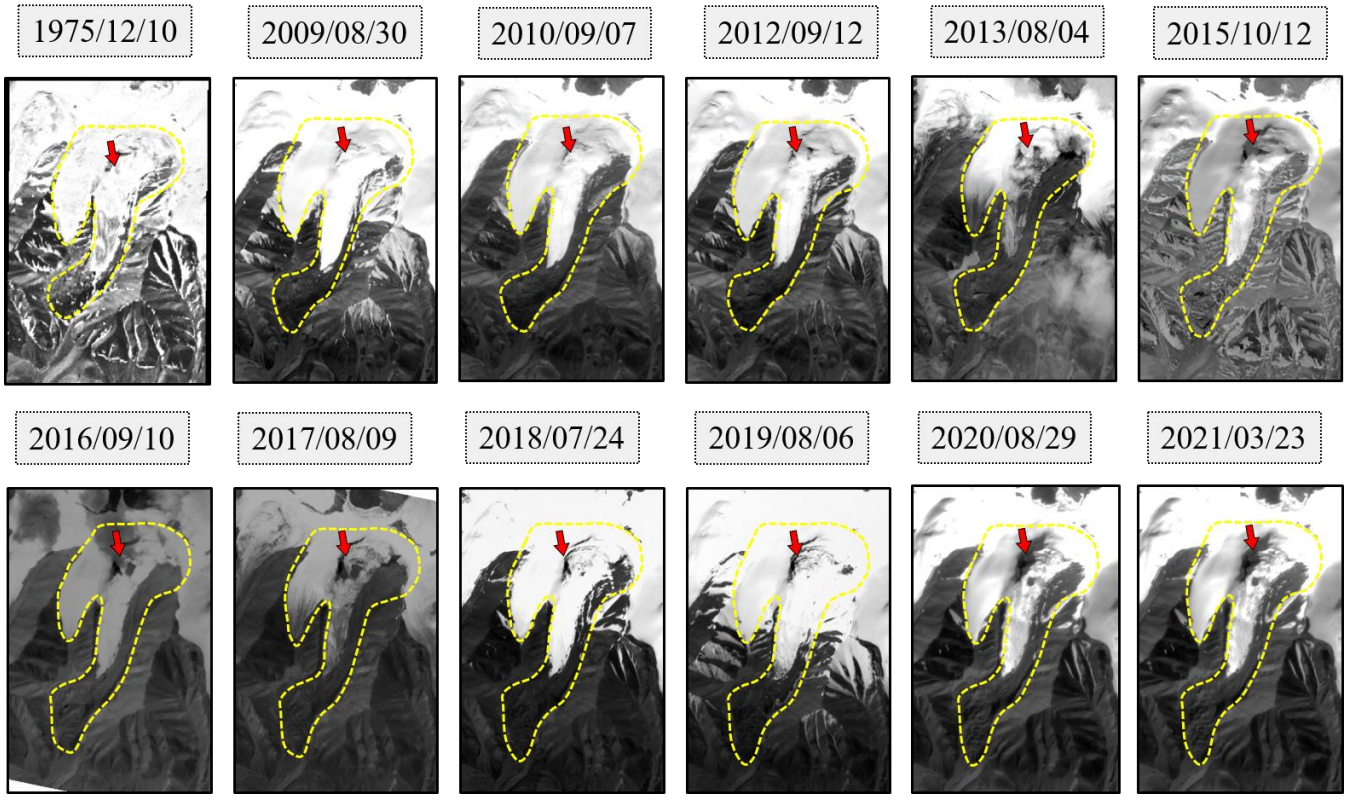

Figure S4: Time-lapse of the Planet optical images covering the full KLP-37 glacier (© Planet Labs). In each image, the yellow polygon outlines the glacier boundary, and the red arrow marks the place where crevasses develop in the glacier cirque.

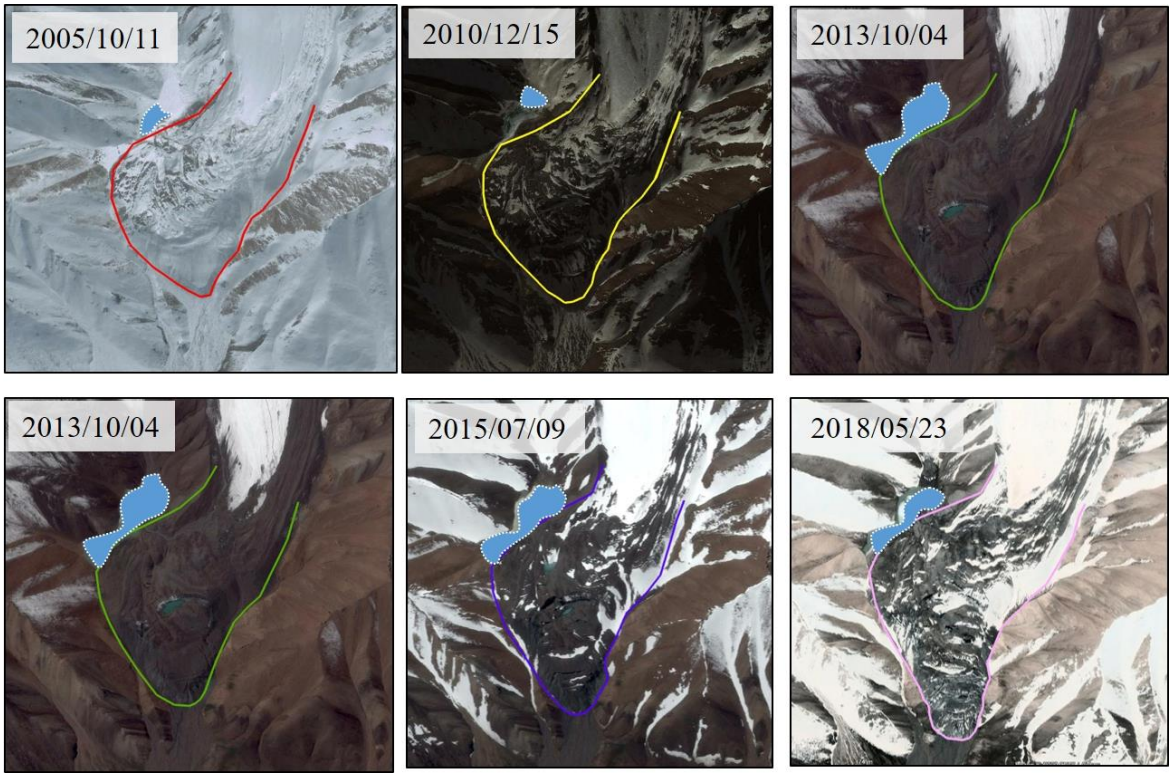

Figure S5: Time-lapse of the high-resolution Google Earth images covering the KLP-37 glacier tongue (© Google Earth™). The light blue polygon in each image delineates the ice-dammed lake, and the colored line indicates the glacier snout boundary.

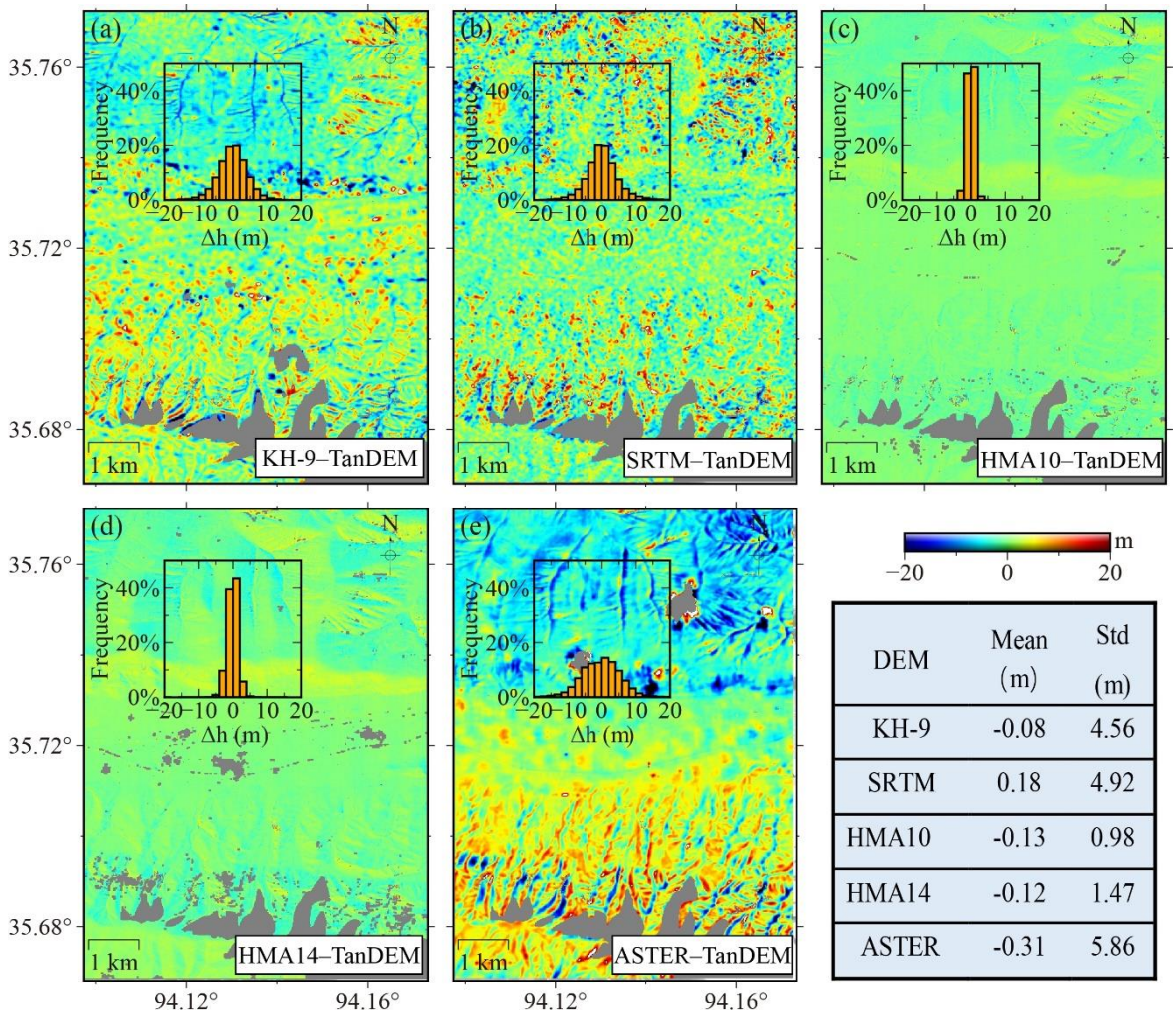

DEM	Mean (m)	Std (m)
KH-9	-0.08	4.56
SRTM	0.18	4.92
HMA10	-0.13	0.98
HMA14	-0.12	1.47
ASTER	-0.31	5.86

Figure S6: DEM differences over the off-glacier region between the (a) KH-9, (b) SRTM, (c) HMA2010, (d) HMA2014, (d) ASTER and the TanDEM (i.e., TanDEM-X DEM). The inset histograms show the distribution of elevation differences. The table lists the mean values and standard deviations (std.) of the elevation differences.

Table S1. The area of the ice-dammed lake (see Fig. 3 & Fig. S4 for its location) estimated from optical images.

Image date	Lake area (m^2)	Image source
2005/10/11	6742±505	Google Earth
2006/07/11	15769±1545	Google Earth
2009/08/30	15826±1061	Planet Lab
2010/09/07	19040±1509	Planet Lab
2010/12/15	3745±229	Google Earth
2012/09/12	12761±1117	Planet Lab
2013/07/18	19018±1193	Google Earth
2013/08/04	17558±1322	Planet Lab
2015/07/09	17916±1522	Google Earth
2015/10/12	10069±951	Planet Lab
2016/09/10	17466±1711	Planet Lab
2017/08/09	21276±1646	Planet Lab
2018/05/23	9356±533	Google Earth
2018/07/24	20899±1201	Planet Lab
2019/08/06	17247±1084	Planet Lab
2020/08/29	13543±753	Planet Lab
2021/03/23	7687±896	Planet Lab

Table S2. Changes in coordinates of the KLP-37 glacier terminus point during different periods. Note ΔX and ΔY represent the coordinate offsets in east-west and north-south directions, respectively.

Image pairs	ΔX (m)	ΔY (m)	Distance (m)	Time interval (a)	Velocity ($m \cdot a^{-1}$)
1975/12/10–2009/08/30	-28	213	153±15.26	33.66	4.55±0.46
2009/08/30–2010/09/07	8	-15	17±7.47	1.02	16.64±7.32
2010/09/07–2012/09/12	-22	22	31±7.47	2.02	15.37±3.70
2012/09/12–2013/08/04	8	12	14±7.47	0.89	15.72±8.39
2013/08/04–2015/10/12	-2	33	33±6.31	2.19	15.08±2.88
2015/10/12–2016/09/10	3	30	30±4.87	0.92	32.78±5.29
2016/09/10–2017/08/09	-1	31	31±4.87	0.91	34.08±5.35
2017/08/09–2018/07/24	10	28	30±4.87	0.96	31.37±5.07
2018/07/24–2019/08/06	-5	33	33±4.87	1.04	31.87±4.68
2019/08/06–2020/08/29	11	30	32±4.87	1.06	30.19±4.59
2020/08/29–2021/03/23	4	13	14±4.87	0.56	25.00±8.70